Rend. Fis. Acc. Lincei (2015) 26:25–35
DOI 10.1007/s12210-015-0380-y

Italian seas wave extremes: a preliminary assessment

Mauro Sclavo · Francesco Barbariol · Filippo Bergamasco · Sandro Carniel · Alvise Benetazzo

Received: 30 May 2014 / Accepted: 13 January 2015 / Published online: 18 February 2015
© Accademia Nazionale dei Lincei 2015

Abstract Occasional damages occurring to offshore structures and routing ships have brought attention on whether conventional analyses of stormy seas are adequate to represent wave extremes. Indeed, field and laboratory data showed that in short-crested seas (typical of stormy conditions) the maximum wave elevation is rarely retrieved by a single-point observation (a buoy, for example), which tends to underestimate the actual extreme that occurs over an area surrounding the point. Recently, stochastic models for the prediction of maxima of multidimensional Gaussian random fields (e.g. the Piterbarg's theorem and the Adler and Taylor's Euler Characteristics approach) have been successfully applied to ocean wave statistics, thus permitting to extend the extreme value analysis from the time to the space–time domain. Results from space–time models are here firstly compared to observations gathered by an optical stereo system, and then used to preliminarily assess wave extremes over the Italian Seas, by using a numerical model analysis covering the period 2007–2013. In particular, space–time maxima are estimated as affecting a fishing boat and a cruise ship, showing that, locally, space–time extremes may exceed time-based values up to about 50 %.

Keywords Sea surface waves · Space–time extremes · Stereo vision · Numerical models · Italian seas

1 Introduction

Sea surface waves have been historically observed at fixed points on the sea by using instrumentation apt to gather time evolution of the sea surface displacement from a reference level (conventionally the mean sea level). Thus, for decades, data recorded by wave gauges, ultrasonic instruments, and buoys were used as input for spectral and statistical analyses from which infer general and specific characteristics (e.g., extremes) of sea surface waves. However, especially in stormy conditions, wave crests (assumed orthogonal to the direction of wave propagation) have a finite length, hence point-based data tend to generally underestimate the actual maximal elevation that occur over an area nearby the wave sensor. Indeed, the sea surface elevation η evolves in time t over a 2-D space (x, y), such that $\eta = \eta(x, y; t)$, while the standard models for ocean waves have been mostly developed and validated against data gathered at a fixed point (x_0, y_0). In the latter, time is the only independent variable, i.e., $\eta = \eta(t)$, and wave extremes are represented by the maximum sea surface elevation occurring at a point for a given sea state duration (see for example Dysthe et al. 2008). Limitation of

This contribution is the extended, peer-reviewed version of a paper presented at the Conference "Sustainable management of the Mediterranean", held at "Accademia Nazionale dei Lincei" in Rome on March 21, 2014.

M. Sclavo · F. Barbariol · S. Carniel · A. Benetazzo (✉)
Institute of Marine Sciences, Italian National Research Council (ISMAR-CNR), 30122 Venice, Italy
e-mail: alvise.benetazzo@ve.ismar.cnr.it; alvise.benetazzo@gmail.com

M. Sclavo
e-mail: mauro.sclavo@ismar.cnr.it

F. Barbariol
e-mail: francesco.barbariol@ve.ismar.cnr.it

S. Carniel
e-mail: sandro.carniel@ismar.cnr.it

F. Bergamasco
Department of Environmental Sciences, Informatics and Statistics, Università Ca'Foscari Venezia, Venice, Italy
e-mail: filippo.bergamasco@unive.it

such an approach was firstly discussed by Forristall (2006) who investigated the problem of the air gap below the deck of drilling platforms. Socquet-Juglard et al. (2005) and Forristall (2005) drew similar conclusions by means of numerical simulations of short-crested (stormy) sea states, whereas Forristall (2011) observed space–time wave maxima in laboratory experiments.

To fill this gap, theories developed to estimate maxima of multidimensional Gaussian random fields (Adler 1981; Piterbarg 1996; Adler and Taylor 2007) have recently been applied to ocean wave statistics modeling the sea surface as a random n-dimensional process (such that $n = 1$ for time-dependent data, $n = 2$ for 2-D spatial data, and $n = 3$ for space–time datasets). In this context, 3-D extremes are defined as the maximum sea elevation occurring in a sea state of duration T over a horizontal area of sides X and Y. Piterbarg's model (Piterbarg 1996) was applied to ocean wave analysis by Krogstad et al. (2004), while the Euler Characteristics approach of Adler and Taylor (Adler 1981; Adler and Taylor 2007) was successfully applied by Fedele (2012, hereafter FM) to ocean wave statistics. Validation of such theories requires wave data gathered in time over an area to capture wave dynamics as completely as possible. Synthetic aperture radar (SAR) or interferometric SAR (INSAR) remote sensing provides sufficient resolution for measuring waves only at spatial scales larger than 100 m, while LIDARs (Romero and Melville 2011) retrieve only spatial data. However, the recovered surface geometry may be biased by the space–time priors imposed to process the back-scattered data and the long-range nature of such devices make them insufficient to estimate spectral properties at smaller scales. Nowadays, stereo techniques can be effective for such accurate measurements, which are beneficial for many other applications, such as the validation of satellite data and the estimation of dissipation terms for the correct parameterization of numerical wave models. Indeed, a stereo camera view provides both spatial and temporal data whose statistical content is richer than that of time series retrieved from wave gauges (Benetazzo 2006; Gallego et al. 2011, 2013). However, only in the last two decades or so, this traditional approach to stereo imaging has become suitable for applications in oceanography (see also de Vries et al. 2011; Kosnik and Dulov 2011; Brandt et al. 2010; Mironov et al. 2012) thanks to the advent of high performance computer processors. Space–time wave extremes may also be estimated by using numerical model outputs (Barbariol 2014), assuming that maxima of multidimensional random fields might be retrieved by higher order moments of the directional wave spectrum (Baxevani and Richlik 2004). Along this line, in the present study, we have used a modified version of the Simulating WAves Nearshore (SWAN) model, version 40.85 (Booij et al. 1999; see also http://www.swan.tudelft.nl) to compute space–time wave maxima for the Italian Seas. Spatial surfaces covered by two vessels (a fishing boat and a cruise ship) are assumed as reference areas XY for the computation.

The outline of the paper is as follows: the next section describes the stereo system used to observe the space–time maxima, and the theoretical model used to evaluate them. In Sect. 3, the numerical model implemented to compute space–time maxima is described, verified, and applied to the Italian Seas. Finally, in the last section we recap and discuss the results obtained so far.

2 Observation and estimation of wave extremes

2.1 The sea surface observatory system

Sea wave space–time extremes have been estimated by means of a stereo system (namely Wave Acquisition Stereo System, WASS; see Fig. 1) that provides time sequence of sea surface elevation 2-D maps, that is wave elevations over a given horizontal sea area (Benetazzo 2006; Benetazzo et al. 2012). WASS data have already been used, among others, to assess Euler characteristics of oceanic sea states (Fedele et al. 2012) and space–time features of oceanic sea states (Fedele et al. 2013), and to estimate local phase speeds of high wave crests (Banner et al. 2014). For the purposes of the study, WASS (Fig. 2) was mounted on top the "Acqua Alta" oceanographic platform, located in the northern Adriatic Sea (Italy) about 15 km off the Venice littoral (http://www.ismar.cnr.it/infrastructures/piattaforma-acqua-alta?set_language=en&cl=en). The platform is owned and managed by the Italian National Research Council–Institute of Marine Sciences (CNR-ISMAR) and is a preferential site for observing and

Fig. 1 Example of a stereo system (WASS) installation to measure sea surface waves. The two cameras composing the stereo rig are down-looking and about 2.5 m apart

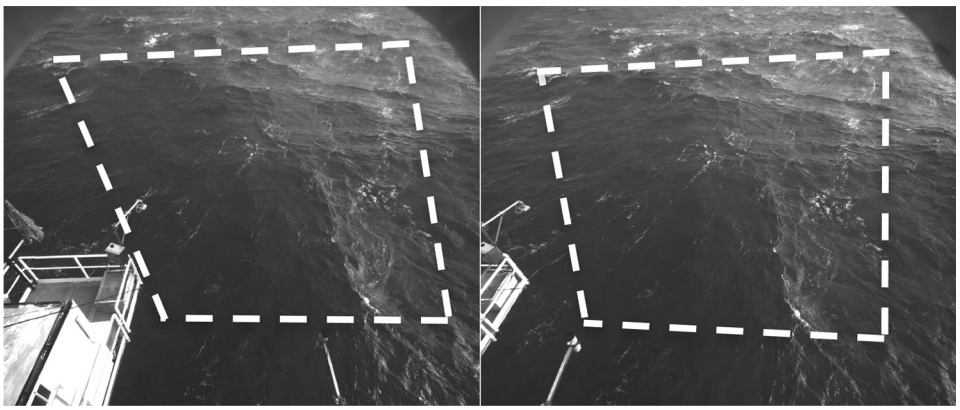

Fig. 2 Example of a WASS snapshot at the "Acqua Alta" platform. Common area between *left* and *right* camera views is edged with a *white dashed line* on both views

assessing atmosphere and sea state parameters (Cavaleri 2000; Benetazzo et al. 2013, 2014a; Barbariol et al. 2013).

WASS used two digital (8-bit monochrome) 2048 × 2456 pixel cameras (model JAI BM-500GE), with uniform pixel size of 3.45 microns, and connected to an external trigger to ensure synchronous grabbing of each image pair. Camera lenses (identical for both cameras) were chosen with focal length equal to 5.0 mm to maximize the cameras overlapping area and minimize the lens distortion and color aberrations. Intrinsic parameters (i.e., focal length, principal point, and distortion parameters) of each camera composing the stereo rig were calibrated by using a handcrafted known target (i.e., a chessboard). Since we expected such target being affected by some imperfections (i.e., printing misalignments, small bumps, or defects) we implemented the method described in Albarelli et al. (2010) that simultaneously optimizes camera parameters and target geometry. Specifically, each stereo camera was internally calibrated independently by acquiring some tens of snapshots of the target with different inclinations and distances from the cameras, spanning a space of about 5 meters depth and 3 meters wide in front of it. The whole set of internal parameters were estimated by imposing zero skewness, square pixels and a 5 coefficients even-degree polynomial radial distortion model. Then, the reciprocal position (i.e., the rotation matrix and the translation vector) between the two WASS cameras was estimated by first recovering the essential matrix using an auto-calibration procedure (Hartley and Zisserman 2003) and then fixing the scale with the known calibration target, as described in Benetazzo et al. (2014). Since we mounted the stereo rig angled with respect to the earth plane, an additional rotation and translation must be estimated to transform the acquired data such that the x–y plane lies on the sea surface with the z-axis facing upward. To estimate this rigid motion, we started by recovering the mean planes of the scattered 3-D data acquired from each frame by means of a robust least square estimation. Then, we averaged the parameters of each plane to obtain a single mean plane that best fits the data throughout

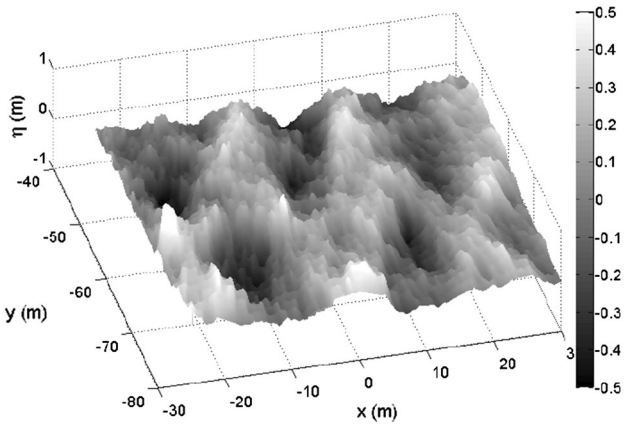

Fig. 3 Example of 2-D wavy water surface elevations $\eta(x, y)$ measured by WASS at "Acqua Alta". The *color bar* displays the water elevation in meters

the whole sequence. Finally, a roto-translation was estimated to align the mean plane with the aforementioned earth-aligned reference system.

An experiment with WASS was conducted at "Acqua Alta" on March 15, 2013 at 11:41 UTC in a crossing-sea wave state, during which southeastern wind conditions (namely "Sirocco") were replacing northeastern winds (namely "Bora"). Wave parameters recorded at "Acqua Alta" provided significant wave height $H_s = 0.58$ m and spectral mean wave period $P = 2.87$ s. WASS dataset consisted of about 6,000 image pairs, acquired at 10 frames per second. WASS configuration and set-up were similar to those used in a previous deployment (Benetazzo et al. 2012) to provide uniform accuracy of about 2–3 cm along the 3-D axes (x and y horizontal, and z vertical). Time records of WASS elevations $\eta(x, y; t)$ (as shown in Fig. 3 for a single snapshot) were filtered in time at 2.0 Hz to remove high-frequency noise and thus analyzed to provide the directional wave spectrum $S(\sigma, \theta)$, shown in Fig. 4, where θ is the wave direction (from geographic North) and σ the angular frequency. The directional spectrum was estimated by applying a stochastic approach, namely the Extended Maximum

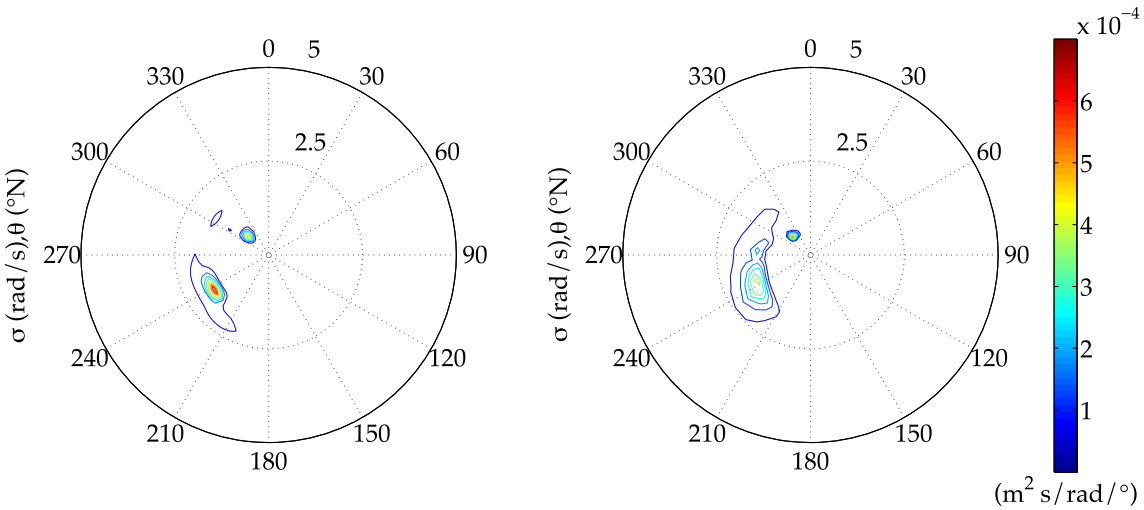

Fig. 4 Observed (*left panel*) and simulated (*right panel*) directional wave spectrum at "Acqua Alta" on March 15, 2013 at 11:41 UTC

Entropy Method (EMEP), applied to a spatial array of virtual wave probes taken in the (x, y) plane of Fig. 3, as in Fedele et al. (2013). The position of the virtual wave probes was randomly chosen in the field and the fulfillment of specific requirements on the relative positions was verified a posteriori (Goda 2000). The EMEP method, that fits the wave data in statistical sense, was demonstrated to reproduce a large variety of directional spectral shape (Benoit et al. 1997). EMEP applicability to stereo data was demonstrated by Fedele et al. (2013) and Barbariol et al. (2014), where EMEP outputs were successfully compared against wave data from reference instrumentation. From the directional spectrum, the angular frequency omnidirectional spectrum given by

$$S(\sigma) = \int_0^{2\pi} S(\sigma, \theta) \mathrm{d}\theta \qquad (1)$$

was used to verify the saturation range of the spectral tail (Fig. 5), that was found consistent with those generally observed for sea wave frequency spectra (Forristall 1981). Also, time sequence of gridded wave elevations $\eta(x, y)$ was analyzed applying a zero-crossing technique in space along the dominant wave direction (as in Romero and Melville 2011). Corresponding spatial wave heights (crest-to-trough vertical distance) are shown in Fig. 6. A general fair agreement has been found between observed data (WASS in Fig. 6) and theoretically expected data, with the Rayleigh distribution acting as an upper bound for the highest waves, which tend to follow Boccotti's law (Boccotti 2000). For the purpose of the work, WASS data were used to prove that the maximum elevation $\eta(x, y; t)$ over an area (XY in Fig. 7) may be up to 40 % higher than the one observable at a point ($XY = 0$). WASS data have provided a sea-truth used to assess theoretical predictions of wave maxima, and numerical model outputs, as described in Sect. 2.2.

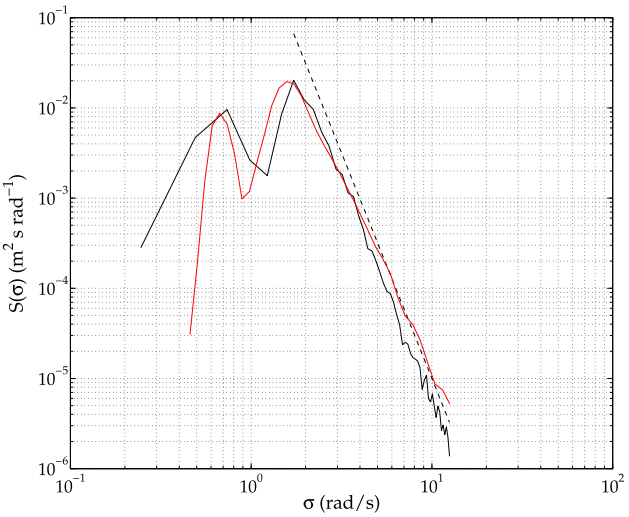

Fig. 5 Observed (*black*) and simulated (*red*) omnidirectional frequency spectrum. Power law proportional to σ^{-5} is superimposed as slope reference (*dashed line*)

2.2 Space–time wave extremes

Prediction of sea surface extremes during a stormy sea state stems from a probabilistic approach. In this context, the sea surface elevation η is treated as a random variable within the sea state, that is the time interval over which the random process can be assumed as stationary (usually 30–60 min or some hours at most). Within the sea state, the asymptotic distribution of maxima relies on the theoretical probability distribution function (pdf), which fits the empirical pdf. Thus, the expected maximum sea surface elevation is defined as the expected value ($\overline{\eta}$) of an asymptotic distribution (Gumbel 1960). As a matter of fact, the time (t) domain is usually considered for investigation

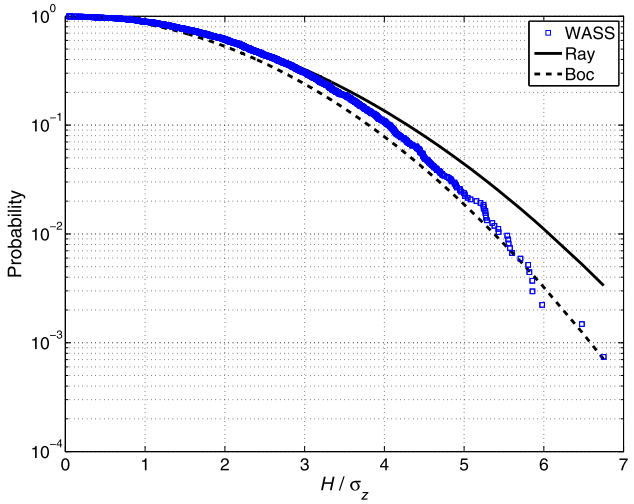

Fig. 6 Exceedance probability of empirical (WASS) spatial wave heights H, normalized with the standard deviation of the wave elevations η (σ_Z). References *curves*: Rayleigh's (Ray) and Boccotti's (Boc) distributions

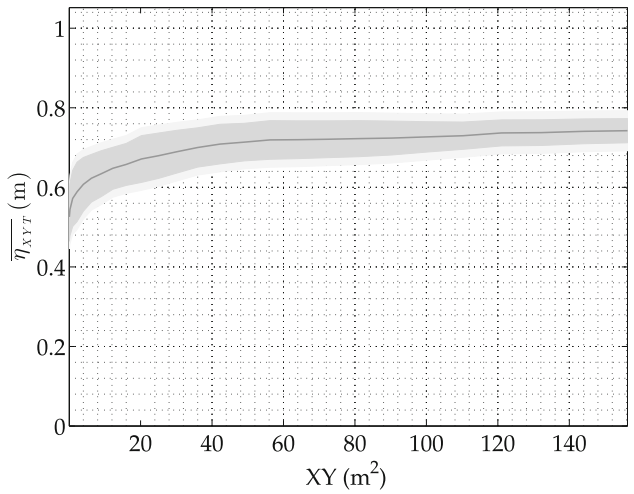

Fig. 7 Observed wave maxima at "Acqua Alta" on March 15, 2013 at 11:41 UTC as function of observed sea surface area XY (taken in the xy domain of Fig. 3). In Figure, the *black line* displays the expected wave maxima, whose uncertainty is shown with a *gray filled area*

of wave extremes. However, in order to provide a more complete representation of wave dynamics, in this paper we extend the analysis to the space–time domain (x, y; t). In the latter, wave extremes are provided by probabilistic models developed to estimate maxima of multidimensional Gaussian random fields. In this context, assuming $\eta(x, y; t)$ normally distributed, the Piterbarg's theorem (Piterbarg 1996) and the Adler and Taylor's Euler Characteristics approach (Adler and Taylor 2007) have been recently applied to ocean wave statistics by Krogstad et al. (2004) and Fedele (2012), respectively.

In order to predict expected maxima in a space–time domain, the leading variable is the wave directional spectrum $S(\sigma, \theta)$, whose integral parameters represent the space–time geometry and kinematics of the sea state (Baxevani and Richlik 2004). These parameters are the mean wave period (P), the mean wavelength and wave crest length (L_x e L_y), and the irregularity parameters of the sea state $(\alpha_{xt}, \alpha_{xy}, \alpha_{yt})$ that are obtained from the spectral moments:

$$m_{ijl} = \int\int k_x^i k_y^j \sigma^l S(\sigma, \theta) \mathrm{d}\sigma \mathrm{d}\theta \tag{2}$$

as:

$$P = 2\pi\sqrt{\frac{m_{000}}{m_{002}}} \quad L_x = 2\pi\sqrt{\frac{m_{000}}{m_{200}}} \quad L_y = 2\pi\sqrt{\frac{m_{000}}{m_{020}}}$$
$$\alpha_{xt} = \frac{m_{101}}{\sqrt{m_{200}m_{002}}} \quad \alpha_{xy} = \frac{m_{110}}{\sqrt{m_{200}m_{020}}} \quad \alpha_{yt} = \frac{m_{011}}{\sqrt{m_{020}m_{002}}} \tag{3}$$

where k_x and k_y are the wavenumber components associated with the wave frequency σ and direction θ. According to the Piterbarg's theorem, the maximum expected sea surface elevation $\overline{\xi}_{XYT} = \frac{\overline{\eta}_{XYT}}{H_s}$ (H_s is the significant wave height) within a sea state of duration T and spatial extension XY is:

$$\overline{\xi}_{XYT} = \left(h_N + \frac{\gamma}{h_N - 2/h_N}\right)/4 \tag{4}$$

where $\gamma \sim 0.5772$, $h_N = \sqrt{2\ln(N) + 2\ln(2\ln(N))}$ and $N = 2\pi\frac{XYT}{L_x L_y P}\sqrt{1 - \alpha_{xt}^2 - \alpha_{yt}^2}$ are the Euler-Mascheroni constant, the modal value in asymptotic distribution of maxima, and the average number of waves within space time domain XYT, respectively. Differently, according to FM, the maximum expected sea surface elevation $\overline{\xi}_{XYT}$ is expressed as:

$$\overline{\xi}_{XYT} = h_0 + \frac{\gamma}{16h_0 - \frac{32M_3h_0 + 4M_2}{16M_3h_0^2 + 4M_2h_0 + M_1}} \tag{5}$$

In Eq. (5), h_0 is the modal value solution of the equation $\left(16M_3h^2 + 4M_2h + M_1\right)\exp\left(-8h^2\right) = 1$, and M_3, M_2, M_1 are the average number of waves within the space–time domain (XYT), on its surfaces (XT, XY, YT), and on the edges (X, Y, T) given by:

$$M_3 = 2\pi\frac{XYT}{L_x L_y P}\sqrt{1 - \alpha_{xt}^2 - \alpha_{xy}^2 - \alpha_{yt}^2 + 2\alpha_{xt}\alpha_{xy}\alpha_{yt}}$$
$$M_2 = \sqrt{2\pi}\left(\frac{XT}{L_x P}\sqrt{1 - \alpha_{xt}^2} + \frac{XY}{L_x L_y}\sqrt{1 - \alpha_{xy}^2} + \frac{YT}{L_y P}\sqrt{1 - \alpha_{yt}^2}\right)$$
$$M_1 = \frac{X}{L_x} + \frac{Y}{L_y} + \frac{T}{P} \tag{6}$$

Piterbarg's theorem and FM differ on the method used to handle the space–time domain boundaries (surfaces and edges). Indeed, Piterbarg's model defines the asymptotic probability of maxima occurring inside the space–time volume and considers populations of completely tridimensional waves evolving over space and time whose spatial characteristic size (represented by L_xL_y) is smaller than XY. Differently, FM takes into account the probability that the maximum can also occurs on the boundaries (i.e. surfaces and edges) of the space–time domain. Thus, FM can also be applied to sea states with spatial sizes larger than XY. As a matter of fact, FM splits into three contributions (M_3, M_2, and M_1) the average number of waves. Also, for sea states and spatial domains such that $X \leq L_x$ an approximation of N was obtained empirically by Forristall (2006) as $N = 2\frac{XT}{L_xP}$.

Piterbarg approach has been verified by means of synthetic wave fields, obtained from numerical simulations. A comparison between expected maxima, theoretically predicted by FM, and observed at sea, is reported in Fedele et al. (2013). In that study, the ratio $\overline{\xi}_{XYT}/\overline{\xi}_T$ for different areas XY was in agreement with WASS stereo-photogrammetric observations, which provided both the directional spectrum $S(\sigma, \theta)$ and the experimental data. A major finding of Fedele et al. (2013) was that the maximum expected over an area could be even 40 % larger than the maximum at a point (similar to what shown in Fig. 7). Additionally, Barbariol et al. (2014) provided a validation of Piterbarg's and Fedele's models, in terms of the expected maximum in space–time $\overline{\xi}_{XYT}$. In Barbariol et al. (2014), WASS observations at the oceanographic tower "Acqua Alta" were exploited to calculate the directional spectrum S of a 600-s sea state, and to estimate the maximum sea surface elevations occurred over XY areas ranging between 0.06 m^2 (comparable to a point-like wave gauge) and 156.25 m^2. Since spatial characteristic features of the sea state were larger than XY for most of the areas considered, Piterbarg's model was applied using Forristall's approximation for all cases where $L_xL_y < XY$. Piterbarg's model and FM were proved to be in general agreement with observations: correlation coefficients between models and observations were 0.96 and 1.00, respectively. Nevertheless, since surface's sides were smaller than wavelengths, FM predictions (Root Mean Square Error RMSE = 0.01 m; best fit line slope $p = 0.93$) were more accurate than Piterbarg's model predictions (RMSE = 0.02 m; $p = 0.79$), despite Forristall's approximation for small areas.

3 Italian Seas wave extremes

3.1 Numerical model setup

In order to assess the Italian Seas wave extremes, we have applied the probabilistic approach described in Sect. 2 to numerical modeling outputs. Indeed, phase-averaged wave models simulate over arbitrary sea domains and states the evolution of the energy spectrum $S(\sigma, \theta)$. The wave spectrum is used to compute wave extremes $\overline{\xi}_{XYT}$ for each computational cell and output time step. To this aim, we have used a modified version of the SWAN (Booij et al. 1999) model, herein called SWAN-ST (where ST stands for space–time; see Barbariol 2014). This model is an extended version of the original code: SWAN-ST preserves all SWAN features, and, in addition, it allows the computation of the integral parameters defined in Eq. (3).

Hence, a SWAN-ST implementation of the central Mediterranean region (i.e. the portion of the basin entailing the seas surrounding the Italian peninsula, as displayed in Fig. 8) was set up in order to simulate 7 years of sea states, covering the period 2007–2013. The domain was discretized with a spatial resolution of 6 × 6 km^2. Model outputs were saved with 1-h time step. ETOPO-1 (http://www.ngdc.noaa.gov/mgg/global/) and GSHHS-H (http://www.ngdc.noaa.gov/mgg/shorelines/gshhs.html) databases were used as source of bathymetric and coastal data, respectively. SWAN-ST was forced by COSMO-I7 (Benetazzo et al. 2013; Russo et al. 2013a, b) high-resolution (7.0 × 7.0 km^2) hourly wind fields. Spectral space $S(\sigma, \theta)$ was discretized using 36 directions equally spaced covering the full circle [0°–360°N] and 39 frequencies belonging to the range 0.05–2.00 Hz. In SWAN, the dissipation source term has been simulated by the formulation suggested by van der Westhuysen et al. (2007), adapted from the expression of Alves and Banner (2003), combined with the wind input term based on the study of Yan (1987). Wave-wave interaction was modeled through DIA (eight fully explicit computations). Bottom friction was modeled according to Madsen formulations (Madsen et al. 1988) using an equivalent bottom roughness length of 0.05 m. Depth-induced wave breaking (Battjes and Janssen 1978) was activated assuming equal to 0.73 the ratio of maximum individual wave height over depth. Numerical scheme employed was backward space-backward time (BSBT).

3.2 Numerical model assessment

An assessment of SWAN-ST results is provided in Fig. 4 where on the right panel the simulated directional spectrum

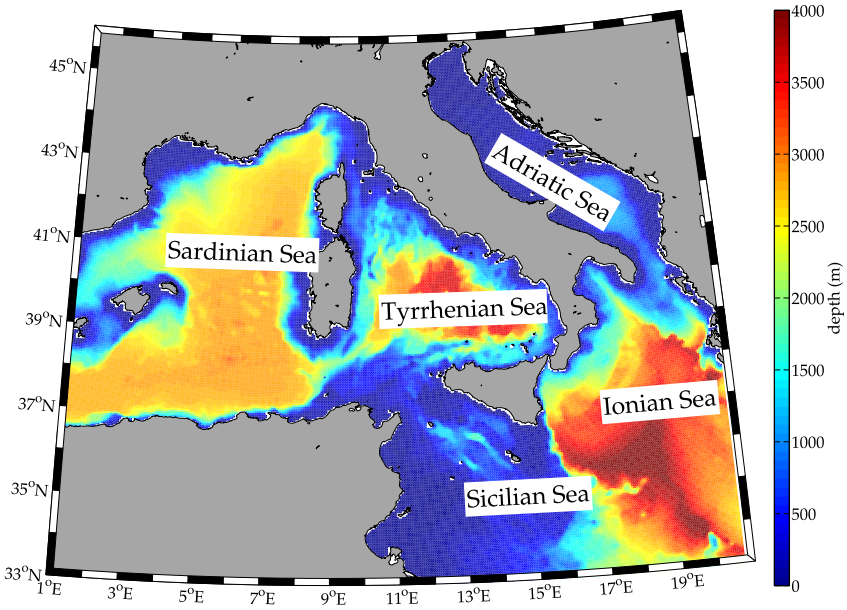

Fig. 8 Computational domain and sea bathymetry of the SWAN-ST numerical model

Table 1 Observed (WASS) and predicted from the observed (EMEP) and simulated (SWAN-ST) directional spectra space–time maxima (according to FM) for different sea surface areas (A) on March 15, 2013 at 11:41 UTC. For the observed values the uncertainty is provided

A = XY (m^2)	$\overline{\eta}_{XYT}$ (m)—WASS	$\overline{\eta}_{XYT}$ (m)—EMEP	$\overline{\eta}_{XYT}$ (m)—SWAN-ST
0.06	0.53 ± 0.08	0.50	0.50
1.00	0.57 ± 0.09	0.55	0.55
9.00	0.63 ± 0.08	0.60	0.60
25.00	0.68 ± 0.08	0.63	0.63
49.00	0.71 ± 0.07	0.65	0.65
100.00	0.73 ± 0.06	0.67	0.67
156.25	0.74 ± 0.05	0.68	0.69

at the time of WASS acquisition is displayed. The crossing-sea state shown in Fig. 4 is well reproduced by the model, as also visible in Fig. 5 where the two energy peaks are shown on both omnidirectional spectra (observed and simulated) with energy levels in fair agreement. Also, space–time extremes $\overline{\eta}_{XYT}$ estimated from observations and model results are shown in Table 1, where, for different sea surface areas XY, the wave extremes are presented as measured within the space–time volume (WASS), calculated from the observed directional spectrum (EMEP), and from the simulated directional spectrum (SWAN-ST). Observed values shown in Table 1 were computed as in Barbariol et al. (2014) selecting different sea areas in the stereo cameras field-of-view and extracting the maximal elevations. Purpose of the data comparison shown in Table 1 is twofold. Firstly, a good agreement between the observed maxima and the extremes estimated from FM applied to the observed directional spectrum indicates that FM is capable of well predicting (albeit in a linear approximation) the dependence of wave extremes by the sea area. On the other hand, the extremes from the simulated spectrum show a similar trend and are in fair agreement with the predictions from observations. These results therefore confirm that the theoretical models are able to predict the actual wave maxima, which are also well reproduced by the simulated wave spectra.

3.3 Italian Seas space–time extremes

To predict Italian sea state extremes in a space–time sense, Eq. (4) of FM was applied. This model was chosen for its generality even for small areas compared to the the characteristic wave size. Time domain extension (T) was chosen equal to 1 h, a typical duration to assume a sea state as stationary. Space domain size (XY) was selected in order to reproduce the sea surface covered by two typical vessels routing the Italian Seas: a fishing boat (the freezer trawler "Illiria" depicted in the upper-left panel of Fig. 9; length: 30 m and beam: 7 m) and a cruise ship (the "MSC Fantasia" depicted in the upper-left panel of Fig. 10; length: 333 m and beam: 38 m). Hence, the areas XY covered by the two ships considered (i.e. $XY = 12{,}654$ m^2 and $XY = 210$ m^2) have been chosen to span the dimension of typical ships routing the Italian Seas: one with a large footprint on the sea (i.e., the

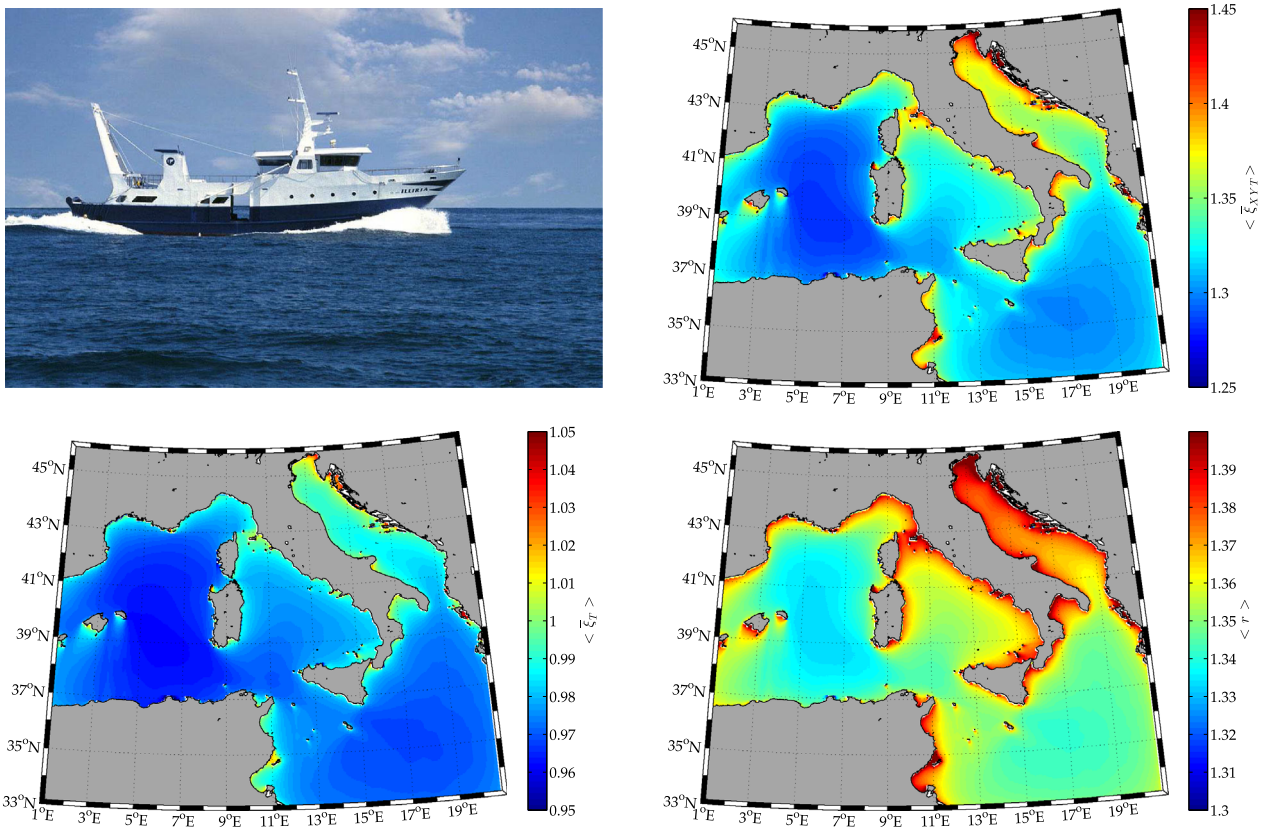

Fig. 9 Results (reference period 2007–2013) of SWAN-ST Italian Seas model and space–time extreme analysis (according to FM) for a fishing ship, the freezer trawler "Illiria" (*upper-left panel*; source: http://www.vittoria.biz/home/en/images/img/fishing/1.jpg). *Upper-right panel* maximum sea surface elevation $\overline{\xi}_{XYT}$ expected over an area $XY = 210$ m^2 and $T = 1$ h. *Lower-left panel* maximum sea surface elevation $\overline{\xi}_T$ expected at a single point inside the area over 1 h. *Lower-right panel* ratio $r = \overline{\xi}_{XYT}/\overline{\xi}_T$. The *symbol* <-> indicates the time-averaging operation

cruise ship) and the other with a smaller one (i.e., the fishing boat). FM estimates of wave maxima were limited by a breaking criterion: maximum allowed steepness was set to $\varepsilon = 0.89/(1 + \psi^*)$, according to Stokes breaking limit and assuming the absolute value ψ^* of the minimum of the autocovariance function equal to 0.75.

Wave maxima at each grid node were time-averaged over the 2007–2013 hourly data and depicted in Figs. 9 and 10. The expected space–time maximal elevations $\overline{\xi}_{XYT}$ over the area XY (210 m^2 in Fig. 9 and 12,654 m^2 in Fig. 10) and time T (1 h) are shown in the upper-right panels. In the lower-left panel, for comparison, the expected time maximum elevations $\overline{\xi}_T$ at a single point are shown. In addition, the spatial contribution is displayed as the ratio r between $\overline{\xi}_{XYT}$ and $\overline{\xi}_T$ (lower-right panels). In general, wave crest time extremes are in the order of H_s ($\overline{\xi}_T = 1$ in the Figures) as expected for a Gaussian sea, with minor differences related to the wave periods typical of the different seas. Space–time extremes, on the contrary, exceed H_s ($\overline{\xi}_{XYT} > 1$), in accordance, also, with the values presented in Table 1.

In particular, results presented in Fig. 9 indicate that a small fishing boat routing the Italian Seas could encounter extreme waves with expected crests elevation $\overline{\eta}_{XYT}$ up to 1.4 times the significant wave height. These values, though surprising, are in agreement with observations of the WASS stereo system at "Acqua Alta" tower, in the northern Adriatic Sea (Fig. 7 and Fedele et al. 2013). Assuming the space–time maxima as the reference value, for a small fishing ship the underprediction of the time-based analysis is approximately 29 %, being the maximum ratio $r = \overline{\xi}_{XYT}/\overline{\xi}_T$ equal to about 1.4. For a cruise ship, results show that the space–time maximum expected wave crests are up to 1.6 times larger than H_s. In this case the underprediction of the time-based model is about 38 %. Regions of the Italian Seas that exhibit the largest $\overline{\xi}_{XYT}$ are the coastal zones and the northern Adriatic Sea. In fact, in shallow waters and fetch-limited zones, the limitation of wavelengths produces a larger number of waves (M_3, $M2$, and M_1 in Eq. 5) and consequently higher probabilities of occurrence of high crests and larger expected crest elevations.

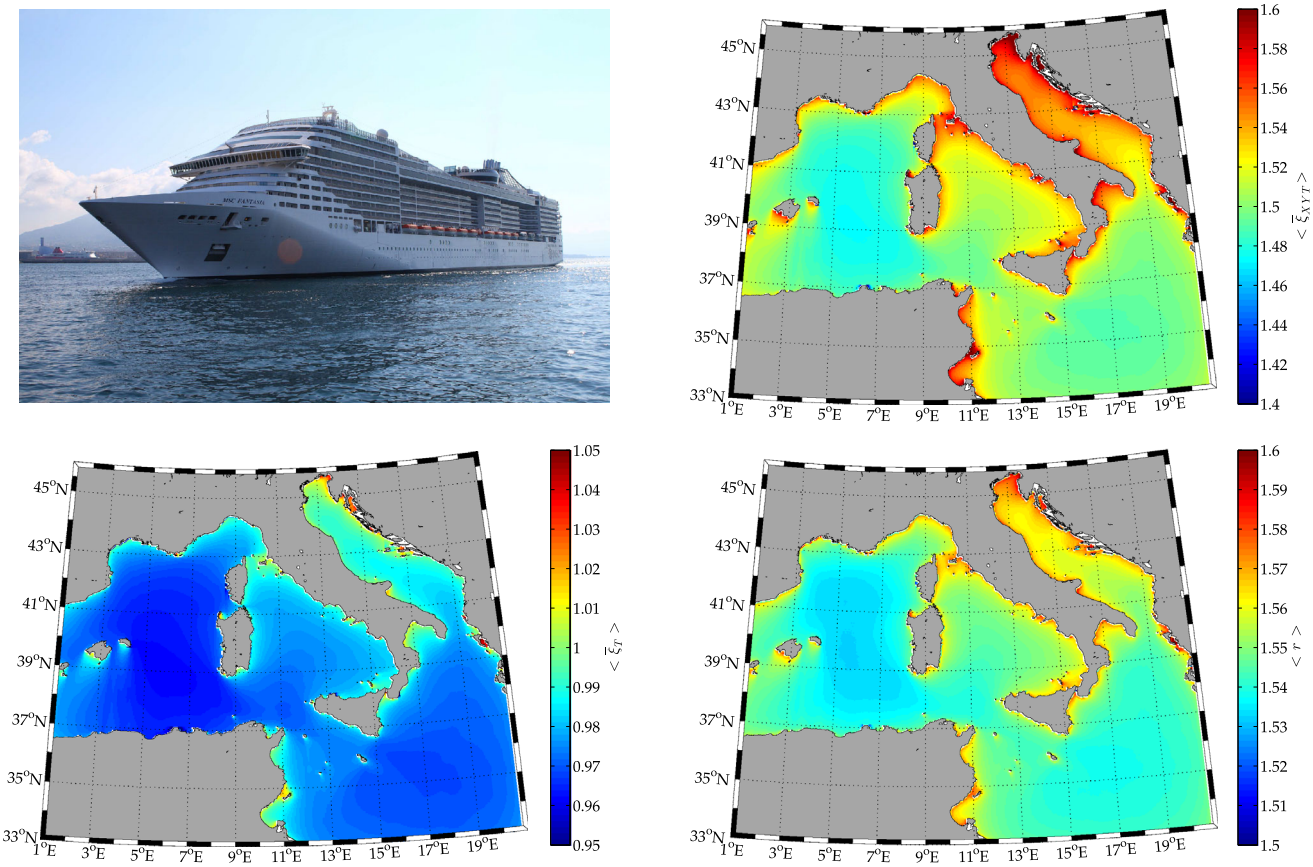

Fig. 10 Results (reference period 2007–2013) of SWAN-ST Italian Seas model and space–time extreme analysis (according to FM) for the cruise ship "MSC Fantasia" (*upper-left panel*; *source* http://it.wikipedia.org/wiki/File:MSC_Fantasia_-_IMO_9359791_(5170241094).jpg). *Upper-right panel* maximum sea surface elevation $\overline{\xi}_{XYT}$ expected over an area $XY = 12{,}654$ m^2 and $T = 1$ h. *Lower-left panel* maximum sea surface elevation $\overline{\xi}_T$ expected at a single point inside the area over 1 h. *Lower-right panel* ratio $r = \overline{\xi}_{XYT}/\overline{\xi}_T$. <-> indicates the time-averaging operation

4 Conclusions

This study has been aimed to provide a first assessment of the Italian Seas space–time wave extremes, by means of a coupling between numerical modeling and space–time probabilistic extreme value analysis. The analysis has used the theories that predict asymptotic maxima of multidimensional random fields in a linear approximation, that has proved to well model these extremes. A sea observatory based on a stereo vision system was used to measure space–time maxima, and showed a fairly good agreement with the expectations from FM. Therefore, this method was herein applied to numerical model outputs reproducing sea wave states of the Italian Seas for the years 2007–2013. Reference sea surface areas have been chosen as representative of a fishing boat and a cruise ship, typical crafts that one can encounter in the Italian Seas. Main findings of the study can be summarized as follows:

- Wave extremes defined in a space–time domain have shown much larger values compared to those derived in the time-domain. This has been proved analyzing the wave data gathered by a stereo camera system that provided time sequence of 2-D maps of the sea surface elevation.
- Space–time maxima over the Italian Seas ranged from about 1.2 to 1.6 times the significant wave height H_s. These values are larger than those provided by a time-analysis.
- Larger maxima attain to the cruise ship that, given its dimensions, is expected to encounter, with higher probability, a larger number of waves and wider portion of wave crests.
- Space–time maxima depend also on the sea states. Fetch-limited sea states (as in the northern Adriatic Sea) provide shorter waves and therefore higher expected waves (compared to H_s).

The analysis performed represents a first step towards an operational system to hindcast/forecast space–time wave maxima along ship routes or offshore structures locations. Results presented show that the inclusions of the space–

time dynamics into the evaluation of wave extremes can lead to higher values that those expected by a traditional approach based on the analysis of time series. Although this is not a completely original result, here we have analyzed the possible consequences of the space–time maxima to nautical structures, such as two different typical ships routing the Italian Seas. Also, a correct modeling of sea state including wave maxima would turn out to be valuable in the field of small-scale processes, such as those related to whitecapping occurrence. Finally, further investigations aimed at shedding light on how oceanic vertical mixing processes are impacted by modified surface wave maxima, and specific assessments of relevance of wave maxima concepts into refined turbulence models (Kantha et al. 2005) are also welcome and desired, since they could as well not be merely local.

Acknowledgments The Authors gratefully acknowledge the funding from the Flagship Project RITMARE—The Italian Research for the Sea—coordinated by the Italian National Research Council and funded by the Italian Ministry of Education, University and Research within the National Research Program 2011–2013, and the Italian Ministry of Research FIRB RBFR08D825 grant (Project "DECALOGO", Coordinator: Sandro Carniel). The authors wish to acknowledge the ARPA-EMR for providing COSMO-I7 meteorological forcings. The SWAN model (version 40.85) was modified under the terms of the GNU General Public License.

References

Adler RJ (1981) The geometry of random fields. Wiley, New York

Adler RJ, Taylor JE (2007) Random fields and geometry. Springer monographs in mathematics. Springer, New York

Albarelli A, Rodolà E, Torsello A (2010) Robust camera calibration using inaccurate targets. BMVC. doi:10.5244/C.24.16

Alves JHG, Banner ML (2003) Performance of a saturation-based dissipation-rate source term in modeling the fetch-limited evolution of wind waves. J Phys Oceanogr 33:1274–1298

Banner ML, Barthelemy X, Fedele F, Allis M, Benetazzo A, Dias F, Peirson WL (2014) Linking reduced breaking crest speeds to unsteady nonlinear water wave group behavior. Phys Rev Lett 112(11):114502–1–114502–5

Barbariol F (2014) Space–time extremes of Sea Wave States: field, analytical and numerical investigations, Ph.D. Thesis, University of Padua (Retrieved from http://paduaresearch.cab.unipd.it/6625/)

Barbariol F, Benetazzo A, Carniel S, Sclavo M (2013) Improving the assessment of wave energy resources by means of coupled wave-ocean numerical modeling. Renew Energy 60:462–471

Barbariol F, Benetazzo A, Bergamasco F, Carniel S, Sclavo M (2014) Stochastic space–time extremes of wind Sea States: validation and modeling. In: Proceedings of the ASME 2014 33rd International Conference on Ocean, Offshore and Arctic Engineering (OMAE 2014) in San Francisco, USA, June 8–13, 2014; paper OMAE2014-23997; pp V08BT06A018; 11 pages; doi:10.1115/OMAE2014-23997

Battjes JA, Janssen JPFM (1978) Energy loss and set-up due to breaking of random waves. In: Proc. 16th Int. Conf. Coastal Engineering, ASCE, pp 569–587

Baxevani A, Richlik I (2004) Maxima for Gaussian seas. Ocean Eng 33:895–911

Benetazzo A (2006) Measurements of short water waves using stereo matched image sequences. Coast Eng 53:1013–1032

Benetazzo A, Fedele F, Gallego G, Shih PC, Yezzi A (2012) Offshore stereo measurements of gravity waves. Coast Eng 64:127–138

Benetazzo A, Carniel S, Sclavo M, Bergamasco A (2013) Wave–current interaction: effect on the wave field in a semi-enclosed basin. Ocean Model 70:152–165. doi:10.1016/j.ocemod.2012.12.009

Benetazzo A, Bergamasco A, Bonaldo D, Falcieri FM, Sclavo M, Langone L, Carniel S (2014a) Response of the Adriatic Sea to an intense cold air outbreak: dense water dynamics and wave-induced transport. Prog Oceanogr 128:115–138. doi:10.1016/j.pocean.2014.08.015

Benetazzo A, Bergamasco F, Barbariol F, Torsello A, Carniel S, Sclavo M (2014b) Towards an operational stereo system for directional wave measurements from moving platforms. In: Proceedings of the ASME 2014 33rd International Conference on Ocean, Offshore and Arctic Engineering (OMAE 2014) in San Francisco, USA, June 8–13, 2014; paper OMAE2014–24024; pp V08BT06A022; 10 pages; doi:10.1115/OMAE2014-24024

Benoit M, Frigaard P, Schäffer HA (1997) Analysing multidirectional wave spectra. In: Proceedings of the 27th IAHR Congress, San Francisco. IAHR Seminar: multidirectional waves and their interaction with structures

Boccotti P (2000) Wave mechanics for ocean engineering. Elsevier Science, Oxford 496 pp

Booij N, Ris RC, Holthuijsen LH (1999) A third-generation wave model for coastal regions: 1. Model description and validation. J Geophys Res 104:7649–7666

Brandt A, Mann JL, Rennie SE, Herzog AP, Criss TB (2010) Three-dimensional imaging of the high sea-state wave field encompassing ship slamming events. J Atmos Ocean Technol 27:737–752

Cavaleri L (2000) The oceanographic tower Acqua Alta—activity and prediction of sea states at Venice. Coast Eng 39(1):29–70

de Vries S, Hill DF, de Schipper MA, Stive MJF (2011) Remote sensing of surf zone waves using stereo imaging. Coast Eng 58(3):239–250

Dysthe KB, Krogstad HE, Müller P (2008) Oceanic rogue waves. Annu Rev Fluid Mech 40:287–310

Fedele F (2012) Space–time extremes in short-crested storm seas. J Phys Ocean 42(9):1601–1615

Fedele F, Gallego G, Yezzi A, Benetazzo A, Cavaleri L, Sclavo M, Bastianini M (2012) Euler characteristics of oceanic sea states. Math Comput Simul 82(6):1102–1111

Fedele F, Benetazzo A, Gallego G, Shih PC, Yezzi A, Barbariol F, Ardhuin F (2013) Space–time measurements of oceanic sea states. Ocean Model 70:103–115

Forristall GZ (1981) Measurements of a saturated range in ocean wave spectra. J Geophys Res Oceans 86(C9):8075–8084

Forristall GZ (2005) Understanding rogue waves: are new physics really necessary. In: Proceedings of the 14th'Aha Huliko'a Hawaiian Winter Workshop, pp 29–35

Forristall GZ (2006) Maximum wave heights over an area and the air gap problem, OMAE2006-92022 paper. In: Proc. ASME 25th Inter. Conf. Off. Mech. Arc. Eng., Hamburg

Forristall GZ (2011) Maximum Crest Heights Under a Model TLP Deck. In: Proceedings of the ASME 2011 30th International Conference on Ocean, Offshore and Arctic Engineering, ASME

Gallego G, Yezzi A, Fedele F, Benetazzo A (2011) A variational stereo method for the 3-D reconstruction of ocean waves. IEEE Trans Geosci Remote Sens 49:4445–4457

Gallego G, Yezzi A, Fedele F, Benetazzo A (2013) Variational stereo imaging of oceanic waves with statistical constraints. IEEE Trans Image Process 22(11):4211–4223

Goda Y (2000) Random seas and design of maritime structures. advanced series on ocean engineering 15, 2nd edn. World Scientific, Singapore

Gumbel EJ (1960) Distributions del valeurs extremes en plusieurs dimensions. Publ. l'Inst. de Statistique. Paris 9:171–173

Hartley R, Zisserman A (2003) Multiple view geometry in computer vision. Cambridge University Press, Cambridge. ISBN 978-0-521-54051-3

Kantha LH, Bao JW, Carniel S (2005) A note on Tennekes hypothesis and its impact on second moment closure models. Ocean Model 9(1):23–29

Kosnik MV, Dulov VA (2011) Extraction of short wind wave spectra from stereo images of the sea surface. Meas Sci Technol 22:1–10

Krogstad HE, Liu J, Socquet-Juglard H, Dysthe KB, Trulsen K (2004) Spatial extreme value analysis of nonlinear simulations of random surface waves. In: Proceedings of the ASME 2004 23rd International Conference on Ocean, Offshore and Arctic Engineering

Madsen OS, Poon YK, Graber HC (1988) Spectral wave attenuation by bottom friction: theory. In: Proc. 21th Int. Conf. Coastal Engineering, ASCE, pp 492–504

Mironov A, Hauser D, Kosnik M, Dulov V, Guerin CA (2012) Statistical characterization of short wind-waves from stereo images of the sea surface. J Geophys Res Oceans 117:C00J35

Piterbarg VI (1996) Asymptotic methods in the theory of gaussian processes and fields, AMS Transl. of Math Monographs

Romero L, Melville WK (2011) Spatial statistics of the sea surface in fetch-limited conditions. J Phys Oceanogr 41:1821–1841

Russo A, Coluccelli A, Valentini A, Paccagnella T, Carniel S, Benetazzo A, Ravaioli M, Bortoluzzi G (2013a) Operational models hierarchy for short term marine predictions: the Adriatic Sea example. In: Proceedings of the OCEANS13 MTS IEEE in Bergen (Norway), June 10–3, paper PID2751753

Russo A, Carniel S, Benetazzo A (2013b) Support for ICZM and MSP in the Adriatic Sea region. Sea Technol 54(8):27–35

Socquet-Juglard H, Dysthe K, Trulsen K, Krogstad HE, Liu J (2005) Probability distributions of surface gravity waves during spectral changes. J Fluid Mech 542(1):195–216

Van der Westhuysen AJ, Zijlema M, Battjes JA (2007) Nonlinear saturation-based whitecapping dissipation in SWAN for deep and shallow water. Coast Eng 54:151–170

Yan L (1987) An improved wind input source term for third generation ocean wave modelling. Scientific report WR-No 87–8. De Bilt, The Netherlands